Advanced Composites and Hybrid Materials (2023) 6:58
https://doi.org/10.1007/s42114-022-00600-5

ORIGINAL RESEARCH

Poly(2-acrylamido-2-methylpropane sulfonic acid)@butyl methacrylate latex anchored into polyethylene glycol diacrylate-based hydrogel composite for drug loading and controlled release studies

Manzoor Hussain[1] · Touseef Rehan[2] · Mazhar Ul-Islam[3] · Omer Shehzad[4] · Abbas Khan[1] · Muhammad Wajid Ullah[5] · Ayesha Baig[6] · Guang Yang[7] · Nasrullah Shah[1]

Received: 24 May 2022 / Revised: 30 October 2022 / Accepted: 4 December 2022 / Published online: 20 February 2023

Abstract

Hydrogels are applied in biomedical fields, especially in sustained drug release studies. However, improvements in their material properties are always needed to make them suitable for their potential biomedical use. Herein, a core–shell particles latex (CS) made of poly(2-acrylamido-2-methylpropane sulfonic acid)@butyl methacrylate anchored into polyethylene glycol diacrylate (PEGDA) matrix-based composite hydrogel (PEG-CS) was prepared through multiple steps free radical polymerization. The fabricated PEG-CS hydrogel was used for the loading and controlled release of ciprofloxacin as a model drug at various experimental conditions. An optimum drug concentration of 30 ppm at a loading efficiency of up to 660 mg/g for PEG-CS hydrogel was obtained after 8 h of adsorption, which was much higher than using only PEGDA-based hydrogel (control). The kinetic models and equilibrium isotherms of adsorption showed that the drug loading followed pseudo-second-order kinetics and the Langmuir adsorption isotherm, respectively. The drug demonstrated a sustained release at 37 °C and pH 7.4, at which 80% of the drug was released after 24 h. The Peppas equation gave "*n*" values of 0.50–0.60, indicating the drug release mechanism was governed by diffusion and erosion processes. The findings of this study show that the fabricated PEG-CS could be an efficient potential material for sustained drug release.

Keywords Water-soluble polymers · Core–shell particle latex · PEGDA-based composite hydrogel · Ciprofloxacin · Sustained release

✉ Guang Yang
yang_sunny@yahoo.com; gyang-hust@hust.edu.cn

✉ Nasrullah Shah
nasrullah@awkum.edu.pk

1 Department of Chemistry, Abdul Wali Khan University Mardan, Mardan 23200, Pakistan

2 Department of Food and Nutrition, Shaheed Benazir Bhutto Women University, Peshawar 45000, Pakistan

3 Department of Chemical Engineering, Dhofar University, Salalah 211, Oman

4 Department of Pharmacy, Abdul Wali Khan University Mardan, Mardan 23200, Pakistan

5 School of the Environment and Safety Engineering, Biofuels Institute, Jiangsu University, Zhenjiang 212013, People's Republic of China

6 Department of Biotechnology, COMSATS University Islamabad, Abbottabad Campus, Abbottabad 22060, Pakistan

7 Department of Biomedical Engineering, Huazhong University of Science and Technology, Wuhan 430074, People's Republic of China

1 Introduction

Hydrogels are materials that hold a significant amount of water owing to the presence of water-retaining groups in their chain ends [1, 2]. These find applications in tissue engineering, contact lenses, wound dressing, and artificial tendons, and the most prominent one is the drug delivery system. The high degree of swelling makes the hydrogel an efficient substance for the controlled release of drugs, and hence, it is a good material to deliver the drug to the specific targeted site [3, 4]. The effective use of a hydrogel for a specific application requires its combination with different other molecules, such as the core–shell particles. For instance, the incorporation of polyethylene glycol (PEG) with core–shell particles has the significance of being biocompatible, cheaper, and noninflammatory, and thus finds numerous applications in the medical field, such as in the preparation of drugs, skin ointments, toothpaste, eye drops, gene therapy, and food additives [5, 6]. Szczęch and Szczepanowicz have

reported the synthesis of core–shell nanoparticles comprising poly(caprolactone), poly(lactic acid), and poly(lactide-co-glycolide) that were used for the loading and targeted delivery of an active molecule coumarin-6 [7]. Core shell of polyaniline nanocomposite with graphene, carbon fiber, carbon tube, and carbon black were further investigated for use in magnetic sensors or information storage devices [8]. Pothen synthesized hybrid core–shell particles comprised of dextran and stearic acid, which were applied for the loading and release of the antiviral drug zidovudine [9]. Al-Kinani et al. also synthesized chitosan-coated core–shell nanocarrier based on magnetic iron oxide nanoparticles and gold nanoparticles, which were applied for the encapsulation and release of curcumin as an anticancer agent with negligible adverse effects on normal cells [10].

It has also been reported that PEG-based core–shell particles can easily cross the blood–brain barrier and deliver the drug, which most drugs cannot pass [11]. Denaturation of a small quantity of proteins has been observed by linking them with PEG, and due to its increased size, the composite can easily pass the blood–brain barrier. Because of such kind of properties, the PEG-based composite is applied as an efficient drug delivery system [12]. All these studies show that PEG incorporated with core–shell particles or PEG-based core–shell particles could be useful for various biomedical applications, especially for developing drug delivery systems.

It has been shown that 2-acrylamido-2-methyl propane sulfonic acid (AMPS) can support the introduction of a large number of molecules due to its high water absorbing and swelling capacity and thus can be useful for biomedical applications [13]. Furthermore, the presence of sulfonate groups like heparin, tissue-like modulus, and high water content make AMPS a suitable biocompatible material [14]. Poly(2-acrylamido-2-methyl propane sulfonic acid) (polyAMPS) has electrostatic repulsion between the ions of similar nature, which causes expansion in the polymeric network structure over a series of pH range from 2 to 12 [15]. A copolymer of polyAMPS with other polymers has been applied for in vitro release of folic acid, insulin, amoxicillin, and doxorubicin [16–19]. Many biodegradable polymers, such as poly(lactic acid), poly(glycolic acid), and poly(lactic-co-glycolic acid), have been used in the synthesis of core–shell materials for the delivery of drugs due to their biocompatible nature. These materials have been used for the incorporation of proteins, antibiotics, anti-cancer drugs, and DNA [20–22]. These core–shell materials have the ability to penetrate hydrophilic molecules through polymeric shells, due to which the release of the drug occurs through the degradation kinetics of biodegradable polymers. However, the drug release is adjusted through variations in the polymeric shell composition as well as the molecular weight [23, 24]. In many cases, the release of the incorporated drug takes from a few hours to several days when some kind of small-sized molecules are incorporated [25–27]. To solve this problem of a faster drug release rate with no side effects of the core-shells, we herein prepared core–shell particles and incorporated them with PEG to make them biocompatible for a longer extended drug release.

Poly(AMPS) has been shown to prevent the formation of blood vessels when analyzed with human umbilical vein endothelial cells. Herein, the incorporation of pro-angiogenic growth factors into the sulfonate groups of poly(AMPS) causes nutrient deficiency and leads to cell death [28, 29]. The structure of poly(AMPS) provides a favorable environment for the loading of a high amount of drug; however, its aqueous soluble nature causes the retention of the drug for a longer period than required and hence hinders the sustained drug release. Moreover, its water-soluble nature may also lead to its release from the body with water. To cope with the issue, we incorporated the poly(AMPS) shell with an emulsion polymerized core of butyl methacrylate (BMA) having hydrophobic nature. It is assumed that the core of BMA would entangle the poly(AMPS) with itself, and as a result, it could retain the drug more effectively without compromising the integrity of the water-soluble poly(AMPS) shell. In the drug delivery systems, the development of advanced pharmaceutical techniques and excipients is improving drug delivery knowledge and applications. The drug can be delivered through different controlled fashions, e.g., immediate release [30], sustained release [31], and biphasic release [32], in terms of controlled release rate, targeted release, topical release, and colon release in terms of controlled release [33]. A wide variety of drug delivery systems (DDSs) made of polymers, lipids, and hydrogels have been developed to meet such requirements. These DDSs typically include polymeric nanoparticles, nanocapsules, liposomes, micelles, nanoemulsions, and nanofibers [34, 35]. Among them, hydrogels are popular for fabricating advanced DDSs, thanks to their capability of manipulating drug loading and release [36].

The use of core–shell particles may sometime have a limitation of non-biocompatibility and clearance rate. PEG is one of the most widely used biocompatible polymers that can be anchored with most polymers and has a good clearance rate. Therefore, in the present study, core–shell particles made of BMA core and of polyAMPS shell have been synthesized as reported in our previous study [37]. To transform the latex form into a hydrogel-based composite material, the core–shell latex was incorporated into the PEGDA matrix to obtain the core–shell particles incorporated-PEGDA-based hydrogel composite (PEG-CS) through a photo-initiation reaction. The as-prepared PEG-CS composite was then characterized and applied for loading and sustained release of ciprofloxacin as the model drug.

2 Experimental

2.1 Synthesis of PEG-based hydrogel composite

The synthesized CS latex in various amounts of 1 to 7 mL was taken in a beaker, followed by the addition of PEGDA-700 in various amounts (1 to 3 mL), and sonicated for 15 min. The photo-initiator 2,2-dimethoxy-2-phenyl acetophenone (0.015 g) was dissolved in 1.5 mL distilled water was added to it, and the mixture was sonicated again. The mixture was then transferred to a petri dish and kept under the 500-W light in the N_2 atmosphere for 30 min, converting the mixture to composite hydrogels. The details of the mixing ratios of the mentioned components in the procedure are given in Table S1.

2.2 Swelling behavior of PEGDA and PEG-CS

The synthesized composite hydrogels were weighed and kept in distilled water for 24 h for determining their swelling behavior. The swelled composite hydrogels were taken out of the water, and the surface water was wiped off with filter paper. The percent swelling was determined by using Eq. (1) [38].

$$q = \left(\frac{W2 - W1}{W1}\right) \times 100 \tag{1}$$

where W_2 is the weight of wet/swollen hydrogel/PEG-CS and W_1 is the weight of dry hydrogel/PEG-CS.

2.3 Loading and controlled release studies of ciprofloxacin

The fabricated PEG-CS hydrogel was used for loading ciprofloxacin as a model drug. Briefly, 100 ppm of the stock solution of the drug was prepared [39, 40] and diluted to 20 ppm. Each hydrogel (0.1 g) was added to a separate 20 ppm solution of the drug at 278 K temperature. The flasks containing the mixtures were kept in a shaker for 24 h. The amount of the drug was calculated by determining the absorbance via a UV–vis spectrophotometer. The loading of the drug was optimized at various pHs, times, and amounts of hydrogel.

The drug-loaded hydrogel composites were further investigated for the release of incorporated drug at 37 °C in the presence of phosphate buffer saline (PBS) of pH 7.4. For this purpose, the pre-weighted PEG-CS, after loading with the drug, was put into 20 mL of buffer for 24 h, and the release of the drug was measured by taking 2 mL from the desorption solution at an interval of 0.5, 1, 2, 3, 4, 8, and 24 h. The absorbance of collected samples was determined via a UV–vis spectrophotometer to determine the concentration of the solution after the specified intervals.

2.4 Kinetic study of adsorption and intra-particle diffusion study

The data obtained from the results were interpreted by using a pseudo-first-order kinetic model according to Eqs. (2) and (3).

$$Log\ (qe - qt) = Logqe - \frac{K1t}{2.303} \tag{2}$$

$$qe\ or\ qt = (Ci - Ce)\frac{V}{n} \tag{3}$$

where V is the solution (25 mL) of the drug used, m is the mass of the hydrogel (0.1 g) taken, Ce is the final drug concentration, Ci is the drug concentration initially used, $K1$ is the rate constant in the equation for first order, qt is the quantity of the drug loaded at any time, and qe is the quantity of the drug loaded at the time of equilibrium (8 h).

Similarly, the obtained adsorption data was further interpreted by using the second-order kinetic model according to Eq. (4).

$$^{t}/_{qt} = {}^{t}/_{qe} + {}^{1}/_{qe^2} \tag{4}$$

where qe is the quantity of drug loaded at equilibrium, qt is the quantity of the loaded drug at any time, and $k2$ is the rate constant for second-order.

The resistance of intra-particle diffusion, which affects adsorption, can be explained with the help of the intra-particle diffusion model, as stated below in Eq. (5).

$$qt = Kint\ t^{1/2} + C \tag{5}$$

where C is the intercept that is associated with the width of the border layer, i.e., the higher the value of C, the further its boundary layer outcome.

2.5 Equilibrium isotherm studies

Two isotherms, namely Langmuir and Freundlich, were applied. The Langmuir model was used based on monolayer adsorption of the drug in the hydrogel/PEG-CS composites due to many sites for attachment of the drug. The Langmuir and Freundlich equations are given as Eqs. (6) and (7), respectively.

$$^{Ce}/_{qe} = {}^{1}/_{Kl} + al^{Ce}/_{Kl} \tag{6}$$

where K_L shows the equilibrium adsorption constant while qe is the monolayer loading ability of the drug.

$$Log\ qe = Log\ Kf + {}^{1}/_{n}\ logCe \tag{7}$$

The values for the constants (*Kf* and *N*) of Freundlich and Langmuir (Q and K_L), as well as regression coefficient R^2, were calculated.

2.6 Drug release mechanism investigation using Korsmeyer–Peppas equation

The Korsmeyer–Peppas equation was applied to evaluate the release of the drug from the prepared hydrogels (PEG-CS).

3 Results and discussion

3.1 PEG-based core–shell hydrogel composites (PEG-CS) and their scanning electron microscopy (SEM)

The whole preparation mechanism was completed in three main steps: starting from the synthesis of polyAMPs, then polyAMPs@BMA CS, and finally, the encapsulation of CS into the PEGDA matrix by the photo-initiation reaction that resulted in the formation of PEG-CS composite. The entire chemical reaction process is represented in Fig. 1.

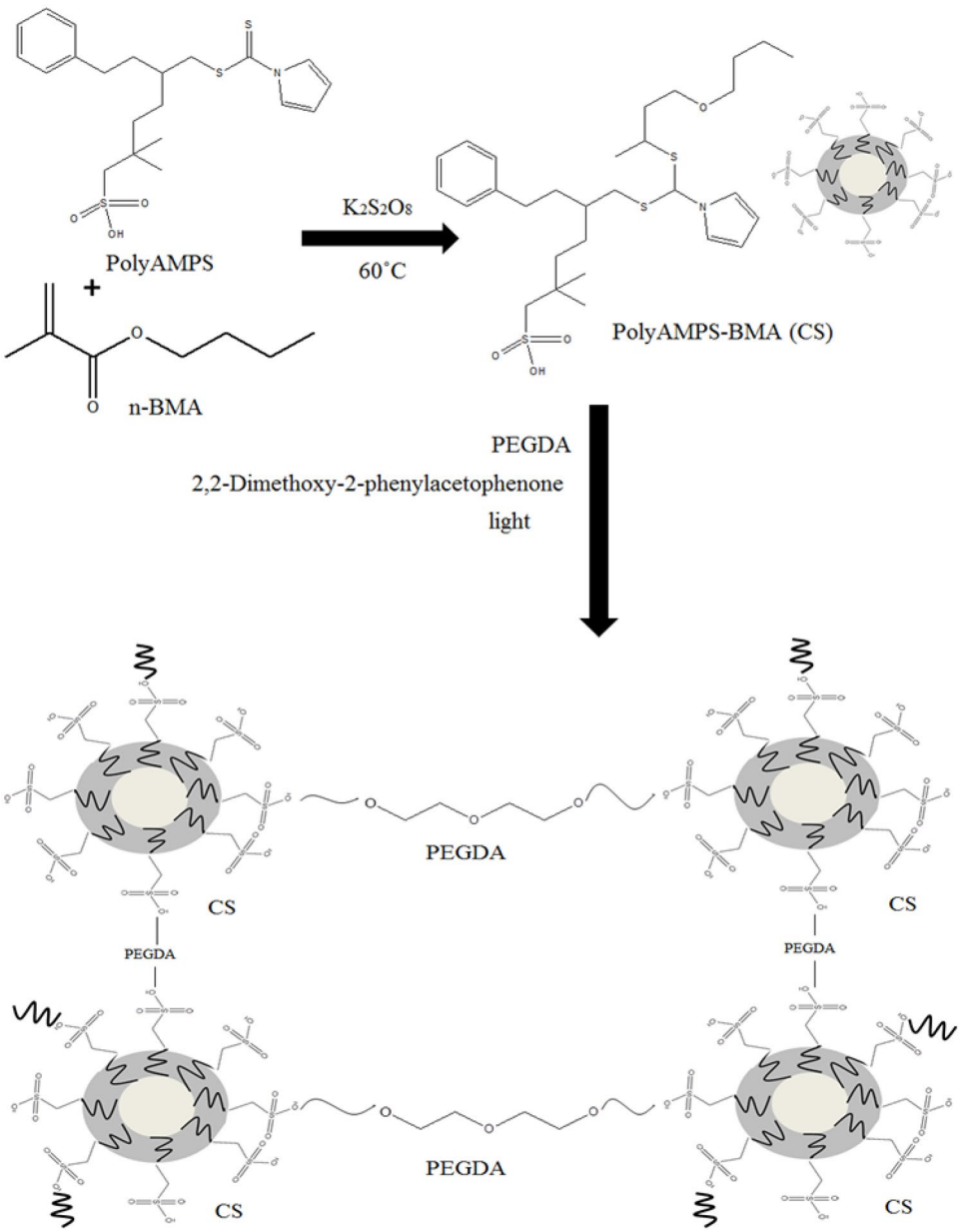

Fig. 1 The chemical reactions process is involved in the fabrication of PEG-CS, whereas in the initial step, polyAMPs are synthesized, followed by the synthesis of polyAMPs@BMA CS, and finally, the cross-linking and encapsulation of the CS into the PEGDA matrix

The PEG-CS formed in disc shapes had a milky-white color, as shown in Fig. 2A. The drying of these hydrogel composites caused them to lose their flexibility and become crystalline and brittle, as evident in Fig. 2B. The brittleness of the hydrogel after drying is due to the loss of water content stored during cross-linking of the core–shell that had provided the slight flexible nature to it. The lowest amounts of PEG and CS needed to produce a composite hydrogel were determined to be 3 and 2 mL, respectively, after the component amounts were optimized. The amount of initiator needed was 0.015 g dissolved in 2 mL of deionized water. In order to evaluate the morphological, topographic, and internal structural characteristics of the as-prepared PEG-CS, SEM analysis was performed. The SEM images shown in Fig. 2C–F reveal that the PEG-CS is porous in nature, where the pores provide sites for the attachment of the loaded drug [41]. Moreover, the images also show that the cross-linking of the CS inside the hydrogels was not uniform, whether these were of the CS itself or even that of PEGDA molecules. Due to this irregular cross-linking of the polymers, the surfaces do not look uniform. Both the virgin PEGDA and PEG-CS hydrogels had rigid surfaces, which is due to the random cross-linking process. Moreover, there is also some debris shown on the surfaces of PEGDA and PEG-CS that might be due to the accumulation of some of the CS latexes on the surface of prepared PEG-CS. The synthesis of the core–shell structure was confirmed by the SEM analysis, as indicated in Fig. 2G. The magnified SEM images in Fig. 2G further confirm the formation of a spherical structure. From the surface structure, it can be concluded that the highly porous nature of the prepared hydrogel makes it a suitable candidate for the loading of a large number of drug molecules. Thus, these hydrogels can be efficient materials in the biomedical field.

3.2 Fourier transform infrared (FTIR) spectroscopy of the PEG-CS

Figure 3A represents the FTIR spectra of the as-prepared PEG-CS. All the PEG-CS have almost similar peaks with very slight variations in the wavelength ranges. This is because all the PEG-CS have a similar composition, with only a difference in the amounts of PEGDA and CS in each PEG-CS. From the obtained spectra, it can be interpreted

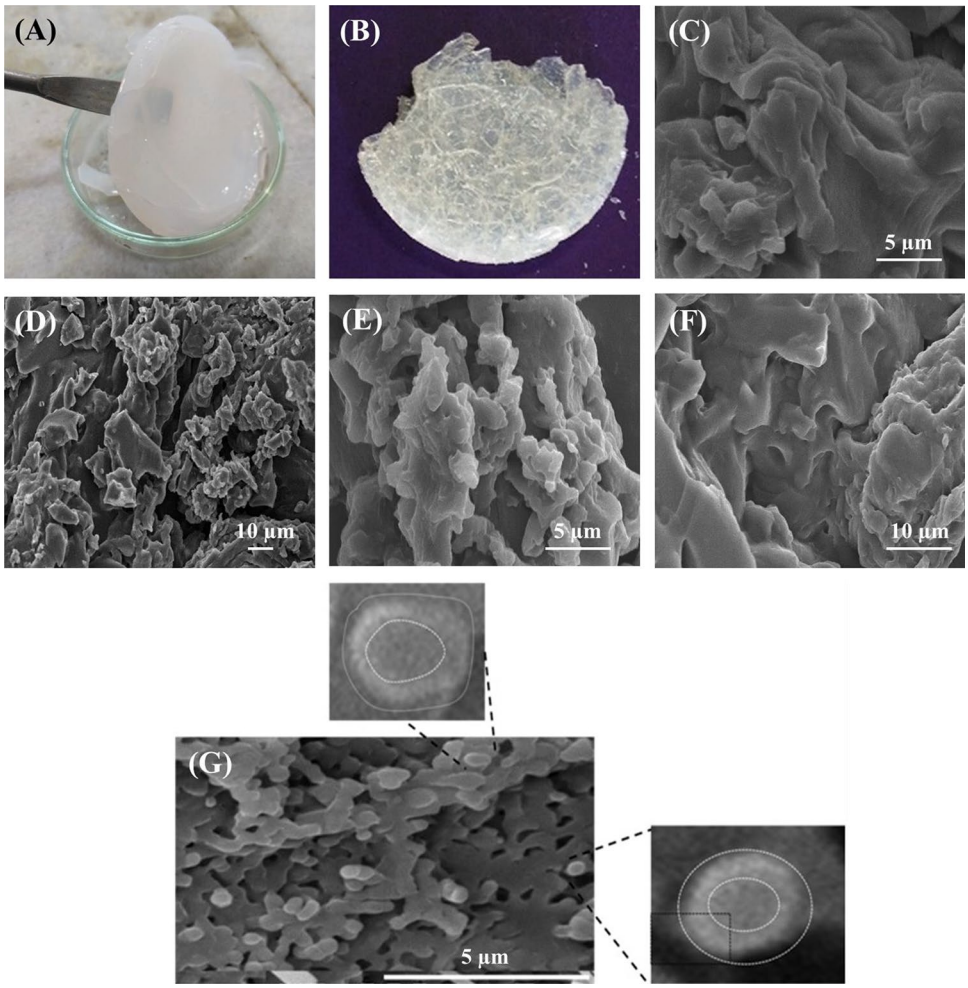

Fig. 2 Digital photographs of the PEG-CS; **A** wet form of PEG-CS and **B** dried PEG-CS, whereas C–F are the SEM images of PEG-CS where **C** PEG5:CS0, **D** PEG3:CS3, **E** PEG3:CS5, and **F** PEG3:CS7, **G** SEM images of prepared CS

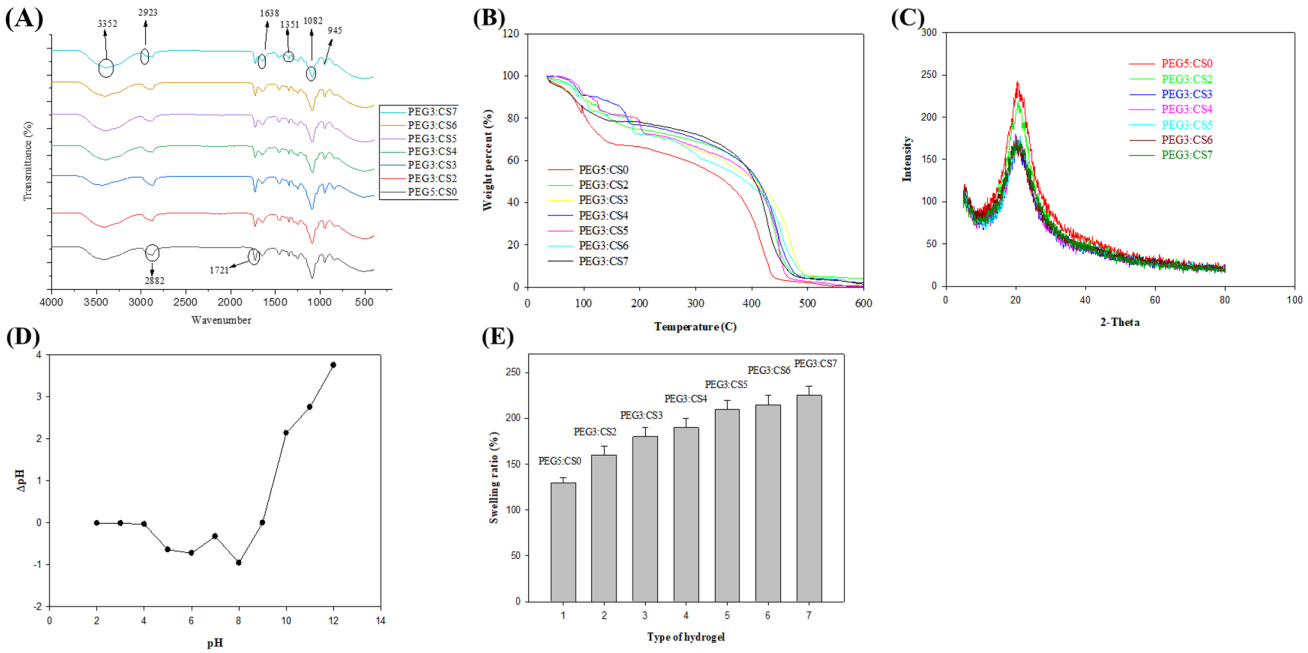

Fig. 3 FTIR spectra of the fabricated PEG-CS prepared by the encapsulation of polyAMPS@BMA into the PEGDA matrix by the photo-initiation polymerization reaction (**A**), TGA of PEG-CS (**B**), XRD of PEG-CS (**C**), pHzpc of PEG-CS (**D**), and the swelling ratio of PEG-CS (**E**)

that the functional groups of the components of the PEG-CS showed their appearance. The peaks at 3352 cm^{-1} represent OH, 2923 cm^{-1} stands for CH, 1721 cm^{-1} shows C = O, 1190 and 1351 are for NH, 1039 cm^{-1} is for SO_2, and 1082 cm^{-1} shows the C-S bond of polyAMPS while the peaks at 1726 cm^{-1} show C = O and 1240 cm^{-1} indicates the presence of BMA [41]. The peak at 2919 cm^{-1} shows CH_2, 1638 cm^{-1} indicates C = C, and 850 cm^{-1} confirms the presence of the CO functional group from the PEG [41].

3.3 Thermogravimetric analysis (TGA) of the PEG-CS

It is clear from Fig. 3B that three degradation stages were observed in the TGA analysis for almost all the fabricated PEG-CS. In the first stage, weight loss occurs at 40 to 150 °C, which is due to the loss of traces of water and other volatile molecules from the PEG-CS. The second degradation stage occurs at 150 to 370 °C, which is due to the loss and or degradation of sulphonic acid groups and PEG chain in the form of SO_2, SO_3, CO, and CO_2 from both control PEG and PEG-CS hydrogels [42]. The third degradation stage happens at 370 to 500 °C that is due to the depolymerization, de-esterification, and denaturation of the polymeric shell of polyAMPs and BMA cores of the PEG-CS and PEGDA hydrogels [42]. Virgin PEGDA hydrogel shows slightly lower thermal stability as it losses water moieties earlier at 130 °C, followed by 50% degradation at 350 °C and then at 450 °C; almost 95% of weight loss occurs that is due to the presence of control PEGDA molecules are cross-linked with each other and break at a lower temperature due to lack of CS as support [43]. From Fig. 3B, it can be observed that the thermal stability of the PEG-CS hydrogels for all composite hydrogels is high, which is due to the possible hydrogen bonds present between the PEG and polyAMPS molecules at the surface of CS as well as between sulfate groups and double bond of PEGDA [44]. From all the data of TGA analysis, it can be said that the incorporation of PEGDA with CS latex of polyAMPS@BMA makes the net composite hydrogel (PEG-CS) thermally more stable, which shows their strength of bonding with each other. Among the various types of PEG-CS prepared, the one containing the larger amount of CS latex had slightly higher thermal stability. The high thermal stability of the CS-incorporated hydrogel suggests that these cannot be degraded easily even at a higher temperature.

3.4 X-ray diffraction analysis of the PEG-CS

The XRD patterns of all the synthesized composite hydrogels (PEG-CS) were evaluated for structural elucidation (Fig. 3C). The peaks at 5.42°, 12.1°, 18.14°, and 20.64° clearly show the amorphous nature of the fabricated hydrogels [45, 46]. There are also very small peaks in the range of 30 to 43° that indicate the crystalline nature to a very smaller extent. There is a significant difference between the peak intensities of the virgin PEGDA hydrogel and PEG-CS hydrogels. PEGDA hydrogel has peaked at 19 to 21° with high intensity, showing a highly crystalline nature. As the

CS was incorporated, the intensity of these peaks decreased, which shifted the PEGDA hydrogel to more amorphous nature; however, the peak positions at 2θ remained the same, showing the cross-linking of PEG with CS. The crystallite size for the prepared hydrogels was calculated through the Scherer equation (Eq. 8).

$$T = \frac{K\lambda}{\beta \cos \theta} \tag{8}$$

where T is the mean particle size of crystallite, λ is the wavelength of the X-ray used, β is the full width at half maximum (FWHM), θ is the angle, and K is a dimensionless shape factor.

After applying Eq. (8), it was found that the mean crystallite size of the control PEGDA hydrogels was 30 nm, while for the rest of the fabricated composite hydrogels, PEG-CS, the mean crystallite size was found to be less than 25 nm. From the calculations, it can be said that the control PEGDA hydrogels have a slightly larger particle size, while PEGDA hydrogels having the CS latex incorporated have a smaller particle size, which makes them suitable candidates for high amounts of drug loading. This decrease in crystal size made available the hydrophilic groups in the polyAMPS chain of the hydrogels. Due to this reason, the drug loading in PEG-CS can be achieved at a higher value than control PEGDA hydrogels.

3.5 Zero-point charge (pHzpc) and swelling ratio of the PEG-CS

The pHzpc result of the hydrogel is given in Fig. 3D. The CS latex is composed of polyAMPS, and its shell contains BMA as its core part. The surface of this composite contains many sulphonate groups containing oxygen on all sides. Oxygen being an electron-rich species, can easily provide it to any of the electron-deficient atom and shifts to cationic form. However, after pH 9 loses those species in the basic media and becomes a negative ion. The pHzpc of the hydrogel was found to be 9. At a pH lower than 9, the hydrogel exists in its cationic form, while at a pH above 9, it exists in anionic form.

The swelling behavior of all the synthesized hydrogels is given in Fig. 3E. The swelling ability of the PEG-CS has improved much compared to the virgin PEGDA hydrogel. This improvement is due to the incorporated CS, which increases the surface area and provides more hydrophilicity to the PEG-CS compared to PEGDA hydrogel. Furthermore, the lower swelling ability of virgin PEGDA hydrogels is due to the regular and packed arrangement of molecules that causes less surface area and the least number of hydrophilic sites for the water to be attached to it [47, 48]. As the CS latex is introduced into the PEGDA, it creates an opportunity for water to adjust and bond with water due to the presence of many sulfate groups of the polyAMPS of CS; hence, the swelling increases to a greater extent. Moreover, increasing the content of core–shell latex has a significant effect on the swelling ability of CS latex with a higher swelling percentage [41, 49]. Along with chemical interactions, this high swelling ability of the fabricated PEG-CS is responsible for the loading and release of the drug.

3.6 Drug (ciprofloxacin) loading on the PEG-CS and its controlled release studies

The loading percent of the drug ciprofloxacin onto the PEG-CS at different times, pHs, and concentrations is given in Fig. 4A–C, while the controlled release pattern of the loaded drug is shown in Fig. 4D. It can be observed that control PEGDA hydrogel has very low loading capacity, which is due to lesser space available for the drug to accommodate inside the hydrogel. It is due to the regular arrangement of PEGDA molecules inside the hydrogels and the lower number of sites available for the attachment of the drug. However, as the PEGDA was incorporated with CS, the sulfate groups of the CS created the opportunity for the drug to be attached to it through hydrogen bonding. The PEG-CS hydrogels with a lower quantity of CS latex contain a smaller number of active sites available for the attachment of the drug than those containing a higher ratio of CS latex. Figure 4A indicates that the loading efficiency for all the PEG-CS hydrogels reached the maximum value of 172 to 261 mg/g until 8 h, and after that, there was no significant increase in the loading of the drug, which is due to the achievement of equilibration.

The pHzpc data of hydrogels (Fig. 3E) show that these are in cationic form at pH less than 9, while these exist in the anionic form above 9. According to Taghavi et al. [50], ciprofloxacin has pka of 6.1 and 8.7, which shows that it exists as a zwitterion in this range. The loading amount of 313 mg/g for control PEGDA hydrogel and 417 mg/g for PEG-CS hydrogel at pH 8 is due to the interaction of positive hydrogel molecules and zwitterion ciprofloxacin molecules. Below pH 9, both the hydrogels and drug have a negative charge, and above pH 9, both show a positive charge. This similar charge causes repulsion between both components in the solution, and hence a low amount of loading takes place. The data of the drug loading at different pH is shown in Fig. 4B and is in agreement with pHzpc data.

The amount of drug loading was also studied based on the concentration of the drug solution used. It is evident from the obtained data shown in Fig. 4C that the increase in the concentration of the drug causes an increase in the loading of the drug. As the concentration of the drug is increased, the amount of drug loaded reaches a maximum value of 439 mg/g for pure PEGDA hydrogel and 660 mg/g for

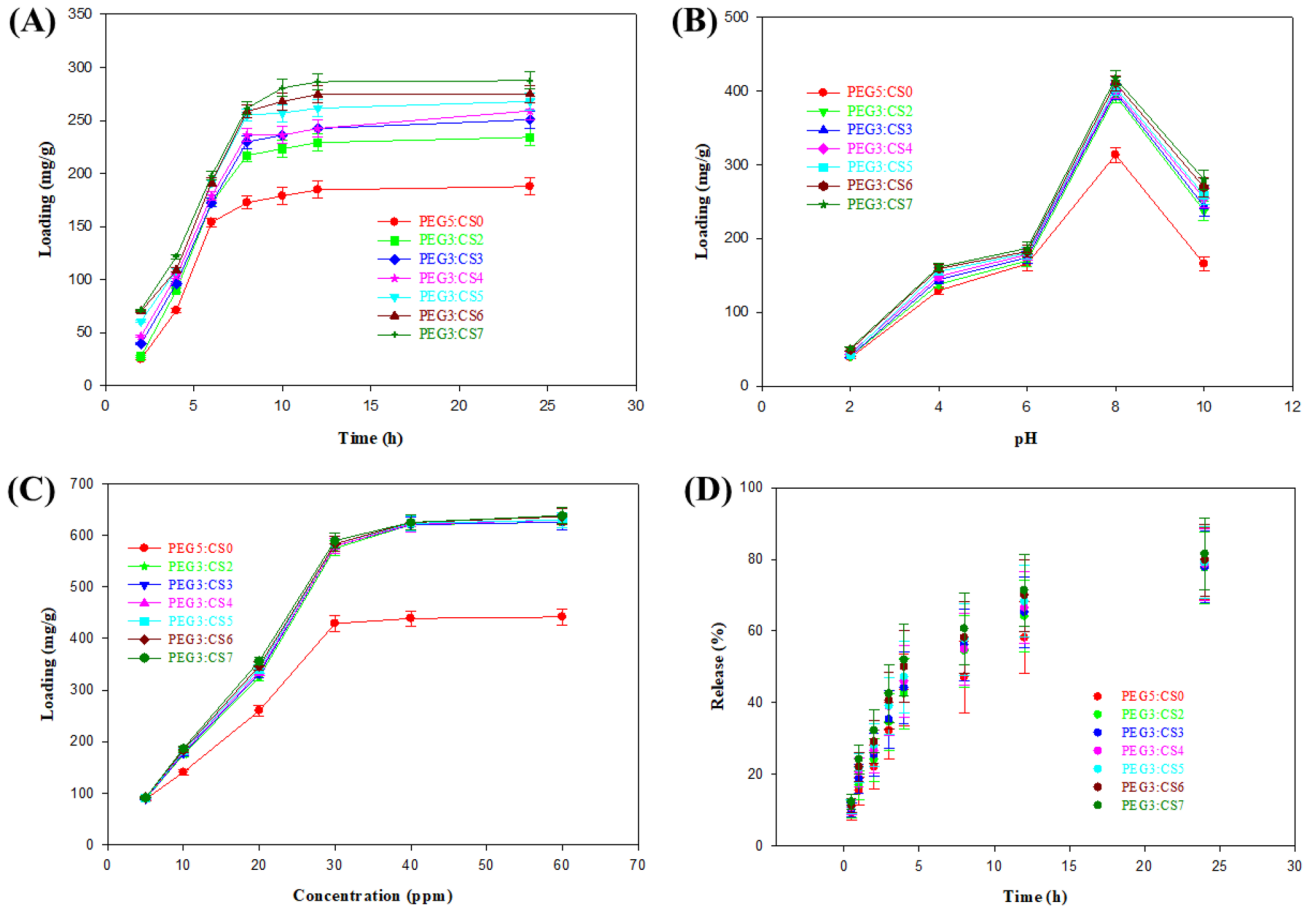

Fig. 4 Loading and release study of ciprofloxacin using the fabricated PEG-CS prepared by the encapsulation of polyAMPS@BMA into the PEGDA matrix by the photo-initiation polymerization reaction. Whereas **A**–**C** are at different times, pHs, and concentrations of the ciprofloxacin solution, respectively, and **D** represents the controlled release pattern of the loaded drug from the PEG-CS in the phosphate-saline buffer at 37 °C

PEG-CS hydrogel. This increase is possibly due to a large number of drug molecules available for attachment with the hydrogel particles. The PEG-CS contains a large number of hydrophilic chain ends, which trap the drug molecules with it and thus increase the chances of loading. Moreover, it can be seen from Fig. 4C that the drug loading is slightly increased when the drug concentration reaches 30 ppm, and after the increase is almost negligible, which gives a clue of the equilibrium between the drug and hydrogels.

The virgin PEGDA and all the fabricated PEG-CS hydrogels were studied for the controlled release of the drug at 37 °C in the presence of a phosphate-saline buffer of pH 7.4. Figure 4D shows that all the PEGDA hydrogels had similar drug release patterns with minor differences due to their basic structural resemblance. In all the cases, the drug release reached 80% after 24 h. The slight differences in the release of the drug for each composite hydrogel are due to the higher content of loading in the composite hydrogels, having a higher content of CS latex incorporated. A similar pattern of controlled release of the drug has also been reported previously [51, 52].

3.7 Evaluation of equilibrium isotherms for adsorption on PEG-CS

The data of adsorption of ciprofloxacin on the as-prepared PEG-CS was further used to analyze the Langmuir and Freundlich isotherms, as shown in Table S2. The data for equilibrium isotherms and their values for loading of ciprofloxacin on PEG and PEG-CS hydrogels is shown in Table S3. Isotherms normally show us the interaction between drug and hydrogel composite. Langmuir adsorption involves monolayer loading of the drug on the homogenous surface of the hydrogel. This model suggests that the surface of PEG-CS has a uniform and a finite number of active sites for the attachment of the drug. The loading of the drug is a favorable process ensured by the value of R^2, which is equal to 1 [53]. Moreover, the value of n in the Freundlich is less than

1, which shows that the loading of the drug does not follow the Freundlich isotherm and satisfactorily follows the Langmuir isotherm [54].

3.8 Evaluation of drug release study by applying the Korsmeyer–Peppas equation

The Korsmeyer–Peppas equation (Eq. 9) was applied to the data obtained for drug release investigation.

$$D = \frac{Q_t}{Q_0} = Ktn \tag{9}$$

where P is the accumulative drug release percentage, Q_t and Q_o are the amounts of drug released into the dissolution medium at time (t) and time (0), respectively, and K and n are the two constants. The values of "n" describe the characteristic of the drug release mechanism [55].

As we know from previous knowledge, the value of "n" gives us information about the drug release mechanism. According to the previous knowledge, the value of "n" less than 0.45 indicates that drug release follows the diffusion mechanism, while higher than 0.90 indicates that drug release follows the erosion mechanism. However, a value in the range of 0.45 to 0.90 shows that drug release is the combination of both diffusion and erosion mechanisms [36, 56]. According to the results in Table S4, the value of "n" is in the range of 0.5 to 0.6, showing that the release of the drug followed a complex mechanism in which both the erosion and diffusion processes are involved. In a more conclusive form, we can say that the release of the drug was due to the irregular and nonuniform cross-linking of the core shell with each other through PEG and the highly swelling capability of the network formed in the hydrogel. These results suggest that the prepared composite hydrogel PEG-CS can be used for the effective sustained release of the drugs.

4 Conclusions

In the present study, we successfully fabricated the hydrogels of virgin PEGDA and PEG-CS through free radical polymerization. The fabrication was confirmed by different analytical techniques, including SEM, FTIR, and XRD analyses. The thermal stability and swelling ratios of the PEG-CS hydrogels were higher than virgin PEGDA hydrogels. The swelling ratio was found to be 130% for virgin PEGDA hydrogel, while for PEG-CS composite hydrogel was 225%. Furthermore, ciprofloxacin was used as a model drug to investigate the loading efficiency of PEG-CS at different pHs, times, and concentrations. Maximum loading was found at pH 8 and a time of 8 h, while it increased with an increase in the concentration of the drug in the solution. The drug-loaded hydrogels were further studied for a controlled release study of the loaded drug at pH 7.4 and 37 °C, and it was found that the release occurs slowly, up to 80% in 24 h. From all the data, it can be said the PEG-CS composite hydrogel, having a high amount of CS latex, is an efficient drug delivery system that can be applied to control the loading and release of the drug.

Supplementary Information The online version contains supplementary material available at https://doi.org/10.1007/s42114-022-00600-5.

Funding This research work was fully supported by the HEC Pakistan under the NRPU project number 20–5201 and partially supported by another project number NRPU-20–3868 awarded to the corresponding author (Prof. Dr. Nasrullah Shah).

Declarations

Conflict of interest The authors declare no competing interests.

References

1. Akhtar MF, Hanif M, Ranjha NM (2016) Methods of synthesis of hydrogels a review. Saudi Pharm J 24(5):554–559. https://doi.org/10.1016/j.jsps.2015.03.022
2. Huang H, Han L, Wang Y, Yang Z, Zhu F, Xu M (2019) Tunable thermal-response shape memory bio-polymer hydrogels as body motion sensors. Eng Sci 9(12):60–67. https://doi.org/10.30919/es8d812
3. Khanum H, Ullah K, Murtaza G, Khan SA et al (2018) Fabrication and in vitro characterization of HPMC-g-poly (AMPS) hydrogels loaded with loxoprofen sodium. Int J Biol Macromol 120:1624–1631. https://doi.org/10.1016/j.ijbiomac.2018.09.184
4. Madhaghiele M, Masullo U, Lionetto MG, Sannino A, Cavallo A et al (2017) Photo-crosslinked poly (ethylene glycol) diacrylate (PEGDA) hydrogels from low molecular weight prepolymer: swelling and permeation studies. J Appl Polym Sci 134(2). https://doi.org/10.1002/app.44380
5. Hussain M, Rehan T, Khan A, Zubair U, Shah N et al (2022) Overview of polyethylene glycol-based materials with a special focus on core-shell particles for drug delivery application. Current Pharmaceutical Design. https://doi.org/10.2174/1381612827666210910104333
6. Zhang J, Zhou J, Zhu X et al (2021) Adsorption characteristics and conformational transition of polyethylene glycol–maleated rosin polyesters on the water–air surface. Adv Compos Hybrid Mater 1–8. https://doi.org/10.1007/s42114-021-00354-6
7. Szczęch M, Szczepanowicz K (2020) Polymeric core-shell nanoparticles prepared by spontaneous emulsification solvent evaporation and functionalized by the layer-by-layer method. Nanomaterials 10(3):496. https://doi.org/10.3390/nano10030496
8. Guo J, Li X, Liu H et al (2021) Tunable magnetoresistance of core-shell structured polyaniline nanocomposites with 0-, 1-, and 2-dimensional nanocarbons. Adv Compos Hybrid Mater 4(1):51–64. https://doi.org/10.1007/s42114-021-00211-6
9. Joshy K, George A, Snigdha S, Joseph B, Kalarikkal N, Pothen LA, Thomas S et al (2018) Novel core-shell dextran hybrid nanosystem for anti-viral drug delivery. Mater Sci Eng C 93:864–872. https://doi.org/10.1016/j.msec.2018.08.015
10. Al-Kinani MA, Haider AJ, Al-Musawi S (2021) Design, construction and characterization of intelligence polymer coated core–shell nanocarrier for curcumin drug encapsulation

and delivery in lung cancer therapy purposes. J Inorg Organomet Polym Mater 31(1):70–79. https://doi.org/10.1007/s10904-020-01672-w
11. Liu L, Guo K, Lu J, Venkatraman SS, Luo D, Ng KC, Ling EA, Moochhala S, Yang YY et al (2008) Biologically active core/shell nanoparticles self-assembled from cholesterol-terminated PEG–TAT for drug delivery across the blood–brain barrier. Biomaterials 29(10):1509–1517. https://doi.org/10.1016/j.biomaterials.2007.11.014
12. Antonsen KP, Hoffman AS (1992) Water structure of PEG solutions by differential scanning calorimetry measurements, in Poly (ethylene glycol) chemistry. Springer. p. 15–28. https://doi.org/10.1007/978-1-4899-0703-5_2
13. Kabiri K, Zohuriaan-Mehr M, Mirzadeh H, Kheirabadi M et al (2010) Solvent-, ion-and pH-specific swelling of poly (2-acrylamido-2-methylpropane sulfonic acid) superabsorbing gels. J Polym Res 17(2):203–212. https://doi.org/10.1007/s10965-009-9306-7
14. Lewis A, Heasysman C et al (2012) Biomedical applications of hydrogels: poly (vinyl alcohol)-based hydrogels for embolotherapy and drug delivery. Polymeric and Self Assembled Hydrogels: From Fundamental Understanding to Applications. Royal Society of Chemistry 232–252. https://doi.org/10.1039/9781849735629-00232
15. Jalababu R, Satya Veni S, Reddy K (2019) Development, characterization, swelling, and network parameters of amino acid grafted guar gum based pH responsive polymeric hydrogels. Int J Polym Anal Charact 24(4):304–312. https://doi.org/10.1080/1023666X.2019.1594058
16. Luo YL, Yuan JF, Liu XJ, Xie H, Gao QY et al (2010) Self-assembled polyion complex micelles based on PVP-b-PAMPS and PVP-b-PDMAEMA for drug delivery. J Bioact Compat Polym 25(3):292–304. https://doi.org/10.1177/0883911510362459
17. Qi X, Wei W, Li J, Zuo G, Pan X, Su T, Zhang J, Dong W et al (2017) Salecan-based pH-sensitive hydrogels for insulin delivery. Mol Pharm 14(2):431–440. https://doi.org/10.1021/acs.molpharmaceut.6b00875
18. Singh B, Sharma V (2016) Designing galacturonic acid/arabinogalactan crosslinked poly (vinyl pyrrolidone)-co-poly (2-acrylamido-2-methylpropane sulfonic acid) polymers: synthesis, characterization and drug delivery application. Polymer 91:50–61. https://doi.org/10.1016/j.polymer.2016.03.037
19. Zhang L, Wang J, Ni C, Zhang Y, Hi GS et al (2016) Preparation of polyelectrolyte complex nanoparticles of chitosan and poly (2-acry1amido-2-methylpropanesulfonic acid) for doxorubicin release. Mater Sci Eng C 58:724–729. https://doi.org/10.1016/j.msec.2015.09.044
20. Nair LS, Laurencin CT et al (2007) Biodegradable polymers as biomaterials. Prog Polym Sci 32(8–9):762–798. https://doi.org/10.1016/j.progpolymsci.2007.05.017
21. Gu B, Sun X, Papadimitrakopoulos F, Burgess DJ et al (2016) Seeing is believing, PLGA microsphere degradation revealed in PLGA microsphere/PVA hydrogel composites. J Controlled Release 228:170–178. https://doi.org/10.1016/j.jconrel.2016.03.011
22. Anderson J, Shive M et al (1998) Biodegradation and biocompatibility of PLA and PLGA microspheres. Adv Drug Deliv Rev 64:72–82. https://doi.org/10.1016/S0169-409X(97)00048-3
23. Dong Y, Su H, Jiang H, Zheng H, Du Y, Wu J, Li D et al (2017) Experimental study on the influence of low-frequency and low-intensity ultrasound on the permeability of the Mycobacterium smegmatis cytoderm and potentiation with levofloxacin. Ultrason Sonochem 37:1–8. https://doi.org/10.1016/j.ultsonch.2016.12.024
24. Frangione-Beebe M, Rose R, Kaumaya P, Schwendeman S et al (2001) Microencapsulation of a synthetic peptide epitope for HTLV-1 in biodegradable poly (D, L-lactide-co-glycolide) microspheres using a novel encapsulation technique. J Microencapsul 18(5):663–677. https://doi.org/10.1080/02652040110055216
25. Chen H, Xie LQ, Qin J, Jia Y, Cai X, Nan W, Yang W, Lv F, Zhang QQ et al (2016) Surface modification of PLGA nanoparticles with biotinylated chitosan for the sustained in vitro release and the enhanced cytotoxicity of epirubicin. Colloids Surf B: Biointerfaces 138:1–9. https://doi.org/10.1016/j.colsurfb.2015.11.033
26. Nguyen TK, Selvanayagam R, Ho KK, Chen R, Kutty SK, Rice SA, Kumar N, Barraud N, Duong HT, Boyer C et al (2016) Co-delivery of nitric oxide and antibiotic using polymeric nanoparticles. Chemical Science 7(2):1016–1027. https://doi.org/10.1039/C5SC02769A
27. Zakeri-Milani P, Loveymi BD, Jelvehgari M, Valizadeh H et al (2013) The characteristics and improved intestinal permeability of vancomycin PLGA-nanoparticles as colloidal drug delivery system. Colloids Surf B: Biointerfaces 103:174–181. https://doi.org/10.1016/j.colsurfb.2012.10.021
28. Liekens S, Neyts J, Degrève B, De Clercq E et al (1997) The sulfonic acid polymers PAMPS [poly (2-acrylamido-2-methyl-1-propanesulfonic acid)] and related analogues are highly potent inhibitors of angiogenesis. Oncology Research Featuring Preclinical and Clinical Cancer Therapeutics 9(4):173–181. ISSN: 0965–0407, 1555–3906 PMID: 9268988
29. García-Fernández L, Halstenberg S, Unger RE, Aguilar MR, Kirkpatrick CJ, San Román J et al (2010) Anti-angiogenic activity of heparin-like polysulfonated polymeric drugs in 3D human cell culture. Biomaterials 31(31): 7863–7872. https://doi.org/10.1016/j.biomaterials.2010.07.022
30. Liu H, Wang H, Lu X, Murugadoss V, Huang M, Yang H, Wan F, Yu DG, Guo Z et al (2022) Electrospun structural nanohybrids combining three composites for fast helicide delivery. Adv Compos Hybrid Mater 1–13. https://doi.org/10.1007/s42114-022-00478-3
31. Liu Y, Chen X, Yu DG, Liu H, Liu Y, Liu P et al (2021) Electrospun PVP-core/PHBV-shell fibers to eliminate tailing off for an improved sustained release of curcumin. Mol Pharm 18(11):4170–4178. https://doi.org/10.1021/acs.molpharmaceut.1c00559
32. Jiang YN, Mo HY, Yu DG (2012) Electrospun drug-loaded core–sheath PVP/zein nanofibers for biphasic drug release. Int J Pharm 438(1–2):232–239. https://doi.org/10.1016/j.ijpharm.2012.08.053
33. Yu DG, Wang M, Ge R (2022) Strategies for sustained drug release from electrospun multi-layer nanostructures. Wiley interdisciplinary Reviews: Nanomedicine and Nanobiotechnology 14(3):e1772. https://doi.org/10.1002/wnan.1772
34. Farboudi A, Nouri A, Shirinzad S, Sojoudi P, Davaran S, Akrami M, Irani M et al (2020) Synthesis of magnetic gold coated poly (ε-caprolactonediol) based polyurethane/poly (N-isopropylacrylamide)-grafted-chitosan core-shell nanofibers for controlled release of paclitaxel and 5-FU. Int J Biol Macromol 150:1130–1140. https://doi.org/10.1016/j.ijbiomac.2019.10.120
35. Sun D, Yan J, Ma X, Lan M, Wang Z, Cui S, Yang J et al (2021) Tribological investigation of self-healing composites containing metal/polymer microcapsules. ES Mater & Manufacturing 14:59–72. https://doi.org/10.30919/esmm5f469
36. Liu X, Zhang M, Song W, Zhang Y, Yu DG, Liu Y et al (2022) Electrospun core (HPMC–acetaminophen)–shell (PVP–sucralose) nanohybrids for rapid drug delivery. Gels 8(6):357. https://doi.org/10.3390/gels8060357
37. Shah N, Khan ZU, Khan A, Hussain M, Rehan T et al (2021) Characterization study of polyAMPS@ BMA core-shell particles using two types of RAFT agents. Materials Science-Poland 39(2):200–208. https://doi.org/10.2478/msp-2021-0015
38. Afroz S, Afrose F, Alam AKMM, Khan RA, Alam M (2019) Synthesis and characterization of polyethylene oxide (PEO)—N, N-dimethylacrylamide (DMA) hydrogel by gamma radiation. Adv Compos Hybrid Mater 2(1):133–141. https://doi.org/10.1007/s42114-018-0058-x

39. Zhou K, Wang M, Zhou Y et al (2022) Comparisons of antibacterial performances between electrospun polymer@ drug nanohybrids with drug-polymer nanocomposites. Adv Compos Hybrid Mater 1–13. https://doi.org/10.1007/s42114-021-00389-9
40. Ahmadi S, Kalaee SAR, Moradi MR et al (2021) Core–shell activated carbon-ZIF-8 nanomaterials for the removal of tetracycline from polluted aqueous solution. Adv Compos Hybrid Mater 4(4):1384–1397. https://doi.org/10.1007/s42114-021-00357-3
41. Clara I, Lavanya R, Natchimuthu N (2016) pH and temperature responsive hydrogels of poly (2-acrylamido-2-methyl-1-propanesulfonic acid-co-methacrylic acid): synthesis and swelling characteristics. J Macromol Sci A 53(8):492–499. https://doi.org/10.1080/10601325.2016.1189282
42. Çakmaklı B, Hazer B, Tekin IO, Comert FG et al (2005) Synthesis and characterization of polymeric soybean oil-g-methyl methacrylate (and n-butyl methacrylate) graft copolymers: biocompatibility and bacterial adhesion. Biomacromolecules 6(3):1750–1758. https://doi.org/10.1021/bm050063f
43. Ponnuvelu DV, Kim S, Lee J (2017) Polyethyleneglycol diacrylate hydrogels with plasmonic gold nanospheres incorporated via functional group optimization. Micro Nano Syst Lett 5(1):1–8. https://doi.org/10.1186/s40486-017-0056-8
44. Çavuş S, Yıldıran M (2016) Poly (ethylene glycol)/poly (2-acrylamido-2-methyl-1-propane sulfonic acid) gel electrolytes: a detailed investigation of their conductivity and characterization. Ionics 22(7):1059–1073. https://doi.org/10.1007/s11581-016-1649-6
45. Kheirabadi M, Bagheri R, Kabiri K (2015) Swelling and mechanical behavior of nanoclay reinforced hydrogel: single network vs. full interpenetrating polymer network. Polymer Bulletin 72(7):1663–1681. https://doi.org/10.1007/s00289-015-1362-z
46. Liu X, Yang K, Chang M, Wang X, Ren J et al (2020) Fabrication of cellulose nanocrystal reinforced nanocomposite hydrogel with self-healing properties. Carbohydr Polym 240:116289. https://doi.org/10.1016/j.carbpol.2020.116289
47. Jafari A, Hassanajali H, Azarpira N, Karimi MB, Miragizadeh B et al (2019) Development of thermal-crosslinkable chitosan/maleic terminated polyethylene glycol hydrogels for full thickness wound healing: in vitro and in vivo evaluation. Eur Polym J 118:113–127. https://doi.org/10.1016/j.eurpolymj.2019.05.046
48. Liu S, Cao H, Guo R, Li H, Lu C, Yang G, Nie J, Wang F, Dong N, Shi J, Shi F et al (2020) Effects of the proportion of two different cross-linkers on the material and biological properties of enzymatically degradable PEG hydrogels. Polym Degrad Stab 172:109067. https://doi.org/10.1016/j.polymdegradstab.2019.109067
49. Zhong S, Sun C, Gao Y, Cui X et al (2015) Preparation and characterization of polymer electrolyte membranes based on silicon-containing core-shell structured nanocomposite latex particles. J Power Sources 289:34–40. https://doi.org/10.1016/j.jpowsour.2015.04.163
50. Najafpoor AA, Sani ON, Alidadi H, Yazdani M, Fezabady AA, Taghavi M et al (2019) Optimization of ciprofloxacin adsorption from synthetic wastewaters using γ-Al2O3 nanoparticles: an experimental design based on response surface methodology. Colloids Interface Sci Commun 33:100212. https://doi.org/10.1016/j.colcom.2019.100212
51. Xie P, Liu P (2019) Core-shell-corona chitosan-based micelles for tumor intracellular pH-triggered drug delivery: improving performance by grafting polycation. Int J Biol Macromol 141:161–170. https://doi.org/10.1016/j.ijbiomac.2019.08.251
52. Bharti S, Kaur G, Gupta S, Tiripathi SK et al (2019) Pegylated CdSe/ZnS core/shell nanoparticles for controlled drug release. Mater Sci Eng: B 243:115–124. https://doi.org/10.1016/j.mseb.2019.03.015
53. Gul S, Shah N, Arain MB, Rahman N, Rehan T, Islam MU, Ullah MW, Yang G et al (2019) Fabrication of magnetic core shell particles coated with phenylalanine imprinted polymer. Polymer Testing 75:262–269. https://doi.org/10.1016/j.polymertesting.2019.02.023
54. Gupta V, Gupta BK, Rastogi A, Agarwal S, Nayak A et al (2011) Pesticides removal from waste water by activated carbon prepared from waste rubber tire. Water Research 45(13):4047–4055. https://doi.org/10.1016/j.watres.2011.05.016
55. Lisik A, Musiał W et al (2019) Conductomeric evaluation of the release kinetics of active substances from pharmaceutical preparations containing iron ions. Materials 12(5):730. https://doi.org/10.3390/ma12050730
56. Liu H, Jiang W, Yang Z, Chen X, Yu DG, Shao J et al (2022) Hybrid films prepared from a combination of electrospinning and casting for offering a dual-phase drug release. Polymers 14(11):2132. https://doi.org/10.3390/polym14112132